Available online at www.sciencedirect.com
SCIENCE DIRECT
Polymer 46 (2005) 7834–7842
polymer
www.elsevier.com/locate/polymer

Incorporation of different crystallizable amide blocks in segmented poly(ester amide)s

P.A.M. Lips[a], R. Broos[b], M.J.M. van Heeringen[b], P.J. Dijkstra[a], J. Feijen[a,*]

[a]*Department of Polymer Chemistry and Biomaterials, Faculty of Science and Technology, Institute for Biomedical Technology (BMTI), University of Twente, P.O. Box 217, 7500 AE Enschede, The Netherlands*
[b]*Core R&D, Dow Benelux NV, P.O. Box 48, 4530 AA Terneuzen, The Netherlands*

Received 22 March 2005; received in revised form 30 June 2005; accepted 5 July 2005

Abstract

High molecular weight segmented poly(ester amide)s were prepared by melt polycondensation of dimethyl adipate, 1,4-butanediol and a symmetrical bisamide-diol based on ε-caprolactone and 1,2-diaminoethane or 1,4-diaminobutane. FT-IR and WAXD analysis revealed that segmented poly(ester amide)s based on the 1,4-diaminobutane (PEA(4)) give an α-type crystalline phase whereas polymers based on the 1,2-diaminoethane (PEA(2)) give a mixture of α- and γ-type crystalline phases with the latter being similar to γ-crystals present in odd–even nylons. PEA(2) and PEA(4) polymers with a hard segment content of 25 or 50 mol% have a micro-phase separated structure with an amide-rich hard phase and an ester-rich flexible soft phase. All polymers have a glass transition temperature below room temperature and melt transitions are present at 62–70 °C ($T_{m,1}$) and at 75–130 °C ($T_{m,2}$) with the latter being highest at higher hard segment content. The two melt transitions are ascribed to melting of crystals comprising single ester amide sequences and two or more ester amide sequences, respectively. These polymers have an elastic modulus in the range of 159–359 MPa, a stress at break in the range of 15–25 MPa combined with a high strain at break (590–810%). The thermal and mechanical properties are not influenced by the different crystalline structures of the polymers, only by the amount of crystallizable hard segment present.

Keywords: Poly(ester amide); Crystallization; Structure–property relations

1. Introduction

Aliphatic poly(ester amide)s, which are biodegradable and have good processing- and end-use properties, are interesting materials for environmental and biomedical applications. Several groups have devoted their research to this class of materials and showed that starting from commercial or synthesized monomers, amide groups can be randomly distributed in the polymer chain or be incorporated in the polymer as well-defined blocks or segments, leading to a wide variety of materials [1–21].

In our previous research, it was shown that the incorporation of well-defined amide blocks or segments in the polyester main chain results in materials with a relatively high melting temperature, a low glass transition temperature and sufficient mechanical properties [20–22]. A strategy to ensure the uniformity of the amide blocks, is the polycondensation of preformed bisamide-diols with aliphatic diesters and diols to obtain segmented poly(ester amide)s.

Bisamide-diols are conveniently synthesized through ring-opening of lactones by α,ω-diamines [4,5,21,24–27]. Polycondensation of such bisamide-diols with dimethyl adipate and aliphatic diols has been intensively investigated [5,7,21,23,28,29]. Poly(ester amide)s are easily prepared but it appeared that bisamide-diols synthesized from diamines and lactide or glycolide are unreactive or decompose at the high polycondensation temperatures. However, this problem is circumvented by performing the polycondensation in solution [27].

Bisamide-diols prepared from 1,4-diaminobutane and ε-caprolactone can be easily incorporated in the polymer chain with hardly any ester amide interchange reactions taking place [21]. The conservation of the bisamide moiety

* Corresponding author. Tel.: +31 534 892 968.
E-mail address: j.feijen@tnw.utwente.nl (J. Feijen).

0032-3861/$ - see front matter © 2005 Published by Elsevier Ltd.
doi:10.1016/j.polymer.2005.07.009

leads to an extraordinary crystallization behaviour of the poly(ester amide)s. The FT-IR and WAXD spectra of these polymers revealed that the crystalline phase shows high spectral similarities to the α-crystalline phase present in nylon 6,6. Moreover, the structural analysis of the bisamide-diol monomer revealed a similarity in crystalline structure of the monomer and polymer, which led to the conclusion that a well-defined segmented polymer is obtained. The crystalline phase therefore is denoted as an α-type crystalline phase. Poly(ester amide)s with a hard segment content >10 mol% show two distinct melting transitions at relative low (58–70 °C) and high (108–140 °C) temperatures which are assigned to the melting of crystals composed of single ester amide sequences and two or more ester amide sequences, respectively.

A bisamide-diol prepared from 1,2-diaminoethane and ε-caprolactone has a completely different crystalline structure than that prepared from 1,4-diaminobutane. The FT-IR and WAXD spectra of this monomer revealed a crystalline structure with structural characteristics of a γ-crystalline phase present in even–odd and even nylons like nylon 6 [31]. The characteristic IR-band of the amide II at 1559 cm^{-1} and the diffraction peak at a *d*-spacing of ~4.2 Å are typical for the structure of even–odd nylons and are found also in the spectra of the bisamide-diol monomer. This prompted us to compare poly(ester amide)s based on these two bisamide-diols and study the relation between their crystalline structure and material properties.

In this paper, the synthesis and properties of segmented poly(ester amide)s prepared from the two different bisamide-diols (Fig. 1) are described. The molar ratio of hard (*x*) and soft (*y*) segment of the poly(ester amide) has been varied by changing the ratio of the alkanediyl-bis[6-hydroxy-hexanamide] to 1,4-butanediol in the condensation with dimethyl adipate. Poly(ester amide)s with a hard segment content of 25 and 50 mol% were selected and their thermal, crystallization and mechanical behaviour were studied.

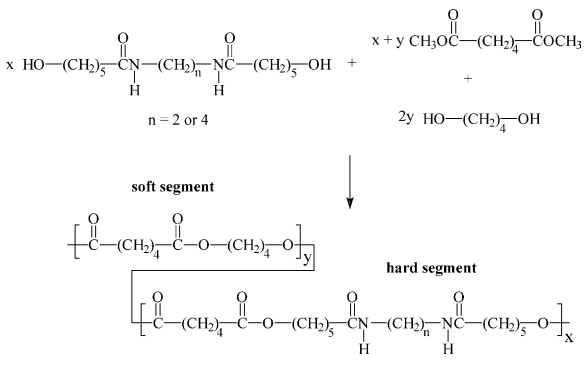

Fig. 1. Reaction scheme for a poly(ester amide) based on bisamide-diol (4) or (2), 1,4-butanediol and dimethyl adipate (PEA(4) or PEA(2)).

2. Experimental

2.1. Materials

1,4-Butanediol, dimethyl adipate (synthetic grade) chloroform-d_1 and the catalyst tetrabutylorthotitanoate ($Ti(OBu)_4$) were purchased from Merck, Germany. The anti-oxidant Irganox 1330 was kindly provided by Ciba Geigi, Switserland. Trifluoroacetic acid-d_1 was obtained from Aldrich, The Netherlands. All other solvents were obtained from Biosolve, The Netherlands. The synthesis of *N*,*N*′-1,4-butanediyl-bis[6-hydroxy-hexanamide] ($T_m=$ 144 °C) and *N*,*N*′-1,2-ethanediyl-bis[6-hydroxy-hexanamide] ($T_m=163$ °C) was described previously [31].

2.2. Poly(ester amide) synthesis

Copolymerisations of *N*,*N*′-α,ω-alkanediyl-bis[6-hydroxy-hexanamide], 1,4-butanediol and dimethyl adipate were performed as previously described [30]. The molar ratio of hard (*x*) and soft (*y*) segments in the poly(ester amide) is varied by changing the ratio of *N*,*N*′-α,ω-alkanediyl-bis[6-hydroxy-hexanamide] and 1,4-butanediol (Fig. 1).

The polymers PEA(4) 72/28, PEA(4) 44/56 with 28 and 56 mol% of *N*,*N*′-1,4-butanediyl-bis[6-hydroxy-hexanamide], respectively, and PEA(2) 74/26 and PEA(2) 49/51 with 26 and 51 mol% of *N*,*N*′-1,2-ethanediyl-bis[6-hydroxy-hexanamide], respectively, were prepared.

2.3. Methods

2.3.1. NMR

^1H (300 MHz) and ^{13}C (75.26 MHz) NMR spectra were recorded on a Varian Inova nuclear magnetic resonance spectrometer using chloroform-d_1 or trifluoracetic acid-d_1 as a solvent.

2.3.2. Viscometry

Intrinsic viscosities [η] were determined by a single point measurement using a capillary Ubbelohde type 0C at 25 °C and a polymer solution with a concentration of 0.1 g dl^{-1} in chloroform–methanol (1:1 vol/vol) [32,33]. The following empirical equation was applied:

$$[\eta]=\frac{\sqrt{2}}{c}\sqrt{\eta_{spec}-\ln\eta_{rel}} \quad (1)$$

where $\eta_{spec}=\eta_{rel}-1$ and *c* is the polymer concentration in g dl^{-1}.

The intrinsic viscosity of PEA(2) 74/26 was also determined by extrapolation of η_{rel} and η_{inh} to $c=0$. According to the previous work, extrapolations were also performed for PEA(4) 72/28 [30].

2.3.3. FT-IR

Fourier transform infrared spectra were recorded with a Biorad FTS 175 spectrometer utilizing a wide band MCT detector at 4 cm^{-1} spectral resolution. Thin polymer films were placed between sodium chloride windows and transferred to a heatable infrared cell from Specac Inc. The sample was heated to 190 °C at 45 °C min^{-1}, kept for 10 min at 190 °C, cooled to 30 °C with an average rate of 5 °C min^{-1}. Subsequently, data points were collected between 4000 and 550 cm^{-1}.

The crystallinity w_c (in mol%) of the poly(ester amide)s was calculated according to:

$$w_c = \left(\frac{b_1}{b_1 + b_2 + b_3}\right)x \tag{2}$$

with b_1 the band area of the amide I band at 1634 cm^{-1} (H-bonded, ordered, crystalline domains), b_2 the band area of the amide I band at ~1651 cm^{-1} (H-bonded disordered, amorphous domains), b_3 the band area of the amide I band at ~1673 cm^{-1} (non-H-bonded, amorphous domains) and x the hard segment content in mol%. Curve fitting was used to resolve the selected IR-band areas.

2.3.4. WAXD

Wide angle X-ray diffraction spectra were recorded using a Philips X'Pert-MPD diffractometer in Bragg–Brentano geometry, with a Θ compensating divergence slit (10.0 mm). The polymer film (15×10×1 mm) was mounted on a Pt filament in an Anton Paar HTK-16 temperature chamber. A Cu-anode was used, together with a curved graphite monochromator, giving Cu Kα_1 radiation of 1.5406 Å. Prior to measurement the chamber was flushed with nitrogen.

The sample was heated to 190 °C, annealed for 10 min and subsequently cooled at 20 °C min^{-1} to 30 °C. Data points were collected in the range of 2Θ is 4–90°.

The peak position at angles of 2θ correspond to interplanar d-spacings according to Bragg's law:

$$d = \frac{n\lambda}{2\sin\theta} \tag{3}$$

with n is an integer and λ is the applied wavelength (1.5406 Å).

2.3.5. TGA

Thermal gravimetric analysis was carried out with 5–10 mg samples under a nitrogen atmosphere in the 50–700 °C range at a heating rate of 10 °C min^{-1}, using a Perkin–Elmer thermal gravimetric analyser TGA-7.

2.3.6. DSC

Thermal analysis of the polymers was carried out using a Perkin–Elmer DSC-7 differential scanning calorimeter equipped with a PE7700 computer and TAS-7 software. Calibration was performed with pure indium. Measurements were performed on isolated precipitated polymers. Samples (5–10 mg) were heated from 25 to 180 °C at a rate of 20 °C min^{-1}, annealed for 5 min, cooled to −80 °C at a rate of 20 °C min^{-1}, and subsequently heated from −80 to 180 °C at a rate of 20 °C min^{-1}. Melting (T_m) and crystallization (T_c) temperatures were obtained from the peak maxima, melt (ΔH_m) and crystallization (ΔH_c) enthalpies were determined from the area under the curve and the glass transition temperature (T_g) was taken at the inflection point. The data presented are determined from the second heating run, unless stated otherwise.

2.3.7. Processing

Compression moulded bars (75×4×2 mm) were prepared with a hot press (THB 008, Fontijne Holland BV, the Netherlands). Polymers were heated for 6–8 min at 20 °C above their T_m as measured by DSC, pressed for 3 min at 300 kN, and cooled in approximately 5 min under pressure to room temperature. Upon compression moulding the intrinsic viscosity of PEA(4) and PEA(2) polymers decreased from ~0.60 to ~0.52 dl g^{-1} and from ~0.95 to ~0.65 dl g^{-1}, respectively.

2.3.8. DMA

Differential mechanical analysis was performed with a Myrenne ATM3 torsion pendulum at a frequency of approximately 1 Hz. The storage modulus (G') and the loss modulus (G'') were measured as a function of temperature. Samples (75×4×2 mm) were first cooled to −100 °C and then heated at a rate of 1 °C min^{-1}. The temperature at which the loss modulus reached a maximum was taken as the T_g. The flow temperature (T_{flow}) was defined as the temperature at which the storage modulus reached 1 MPa.

2.3.9. Tensile test

Tensile tests were conducted with compression moulded bars, cut to dumbbells (ISO 37). A Zwick Z020 universal machine equipped with a 500 N load cell and extensometers was used to measure the stress as a function of strain at a strain rate of 500 mm min^{-1} and a preload of 3 N. Measurements were performed on at least 6 different polymer bars.

2.3.10. Tensile set

Polymer samples (10×10×2 mm), cut from compression moulded bars, were placed between two metal plates at 25 °C (ASTM 395 B standard) and compressed to 75% of their original thickness for 24 h. The sample thickness was determined half an hour after the load was released. The measurements were performed in triplo. The compression set (CS) is calculated according to:

$$\mathrm{CS} = \frac{d_0 - d_2}{d_0 - d_1} \times 100\% \tag{4}$$

where d_0, d_1, and d_2 are the sample thicknesses before, during, and after compression, respectively.

2.3.11. Water uptake

The polymer water absorption was determined by immersing polymer bars (10×10×2 mm) in demineralised water at 37 °C for 28 days. Compression moulded samples were predried at 30 °C under reduced pressure for at least 2 days. The water absorption (wt%) is calculated from:

$$\text{wt\%} = \frac{w_0 - w}{w_0} \times 100\% \quad (5)$$

where w_0 and w are the sample weights before and after treatment, respectively.

3. Results and discussion

3.1. Characterization

In previous research it was shown that segmented poly(ester amide)s are conveniently synthesized by melt polycondensation of dimethyl adipate, 1,4-butanediol and *N*,*N*′-1,4-butanediyl-bis[6-hydroxy-hexanamide] (Fig. 1) [21,22,30]. The incorporation of amide groups in the poly(butylene adipate) main chain has proven to be an excellent method to obtain polymers with enhanced physical and mechanical properties as compared to the polyesters. Similarly, polycondensation of dimethyl adipate and 1,4-butanediol and the bisamidediol *N*,*N*′-1,4-ethane-diyl-bis[6-hydroxy-hexanamide] afforded high molecular weight polymers. The molar ratio of hard (*x*) and soft (*y*) segment in the poly(ester amide)s was varied by changing the molar ratio of the bisamide-diol and 1,4-butanediol in the monomer feed. The poly(ester amide)s are abbreviated as PEA(4) and PEA(2), having 4 and 2 methylene units between the amide groups, respectively.

The thermal and mechanical properties of PEA(4) polymers with a hard segment content of at least 25 mol% are comparable to those of low density polyethylene and are considerably improved compared to the relatively low melting and brittle poly(butylene adipate) [21,22,30]. Therefore, we focussed our research on the poly(ester amide)s PEA(4) 72/28, PEA(4) 44/56, PEA(2) 74/26 and PEA(2) 49/51. The last numbers refer to the molar percentages of soft/hard segment in the corresponding polymers.

Table 1
Chemical composition and physical properties of PEA(4) and PEA(2) polymers

Polymer code	Composition, x[a] (mol%)	M_n[a] (kg mol^{-1})	$[\eta]$[b] (dl g^{-1})
PEA(4) 72/28	28	>50	0.59
PEA(2) 74/26	26	50	1.02
PEA(4) 44/56	56	>50	0.61
PEA(2) 49/51	51	25	0.93

[a] According to ^{1}H NMR.
[b] $CHCl_3$/MeOH (1:1 vol/vol) at 25 °C.

^{1}H NMR was used to estimate the molecular weights (M_n) of the polymers with the assumption that polymer chains have hydroxyl end groups. Care should be taken because polymer chains may exist as macrocycles [34,35].

Due to the inaccuracy in the determination of the integrals of ^{1}H NMR signals corresponding to the end-groups M_n values presented in Table 1 are denoted >50 kg mol^{-1} for the PEA(4) polymers. PEA(2) 74/26 and

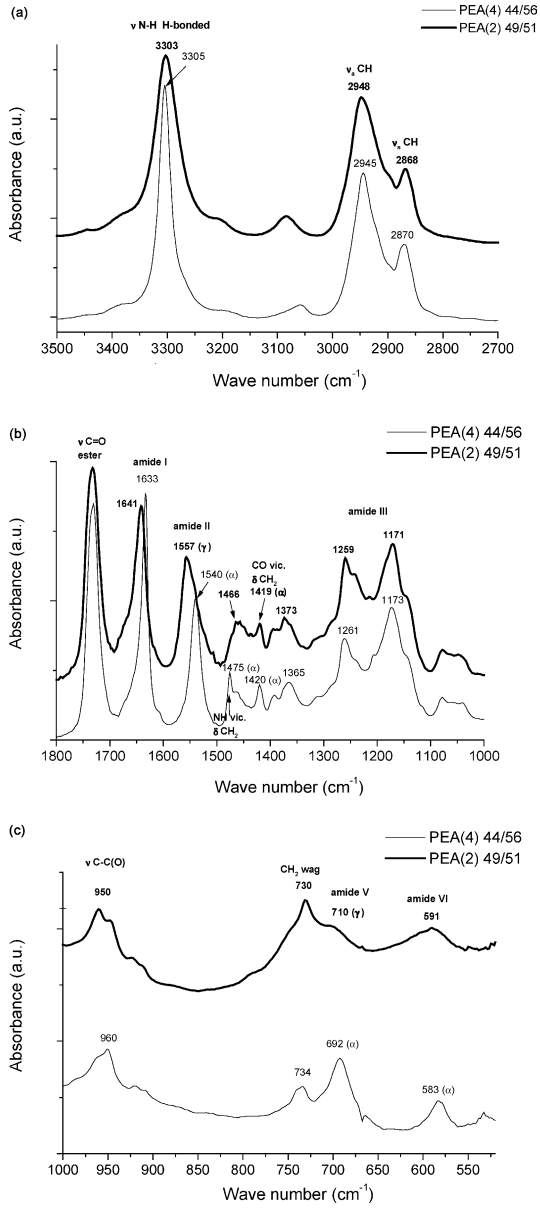

Fig. 2. (a) FT-IR spectra of PEA(4) 44/56 and PEA(2) 49/51 at room temperature for the wave number region 3500–2700 cm^{-1}. (b) FT-IR spectra of PEA(4) 44/56 and PEA(2) 49/51 at room temperature for the wave number region 1800–1000 cm^{-1}. (c) FT-IR spectra of PEA(4) 44/56 and PEA(2) 49/51 at room temperature for the wave number region 1000–525 cm^{-1}.

PEA(2) 49/51 have a M_n of 50 and 25 kg mol^{-1}, respectively.

The composition of the poly(ester amide)s, as determined by ^{1}H NMR, deviates slightly from the intended composition (Table 1). This deviation is caused by distillation of a small amount of dimethyl adipate and the fact that the bisamide-diol is not distilled due to its high boiling point during the polycondensation, which disturbs the stoichiometry.

The polymers PEA(4) and PEA(2) are insoluble in diethyl ether, acetonitrile, toluene and acetone but were soluble in chloroform and DMSO. At elevated temperatures the polymers are soluble in THF and slightly soluble in methanol and ethanol.

Intrinsic viscosities of the polymers were measured by capillary viscometry using chloroform–methanol (1:1 vol/vol) as a solvent (Table 1). This solvent mixture is a good solvent for the PEA(4) 72/28 [30] and PEA(2) 74/26 polymers even at high concentrations, as determined by the reduced ($\eta_{red}=\eta_{spec}c^{-1}$) and inherent ($\eta_{inh}=\ln(\eta_{rel})c^{-1}$) viscosity. As the Mark–Houwink constants are not known for the systems, the resulting intrinsic viscosities could not be converted to molecular weights.

In Fig. 2, the FT-IR spectra of PEA(4) 44/56 and PEA(2) 49/51 at room temperature are presented for the wave number regions, 3500–2700, 1800–1000 and 1000–525 cm^{-1}. Previous work showed that characteristic IR-bands of PEA(4) 44/56 located at 1540, 1476, 1420 and 693 cm^{-1} can be related to an α-type crystalline phase similar to that of the α-crystalline phase of nylon 6,6 [30]. Moreover, for bisamide-diol (4) these characteristic IR-bands are located at the same wave numbers [31], which led to the conclusion that the crystalline structure of the bisamide-diol (4) is preserved in PEA(4) 44/56 [30].

In contrast to PEA(4) 44/56 which shows an amide II band at 1540 cm^{-1}, the amide II band for PEA(2) 49/51 appears at 1557 cm^{-1}. This IR-band is also found for nylon 6 and even–odd nylons and is characteristic of a so-called γ-crystalline phase. Compared to PEA(4) 44/56 (693 cm^{-1}), also the phase sensitive amide V band of PEA(2) 49/51 is shifted to ~710 cm^{-1}, which is characteristic for a γ-type crystalline phase. However, this relatively broad band indicates that an α-type phase is also present, which is confirmed by the presence of a characteristic band of an α-type phase at 1419 cm^{-1}. In addition, the amide II band is very broad which could be due to the presence of the α-related IR-band at ~1540 cm^{-1}.

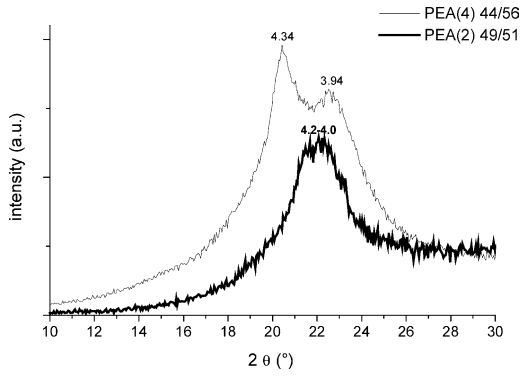

Fig. 3. WAXD spectra of PEA(4) 44/56 and PEA(2) 49/51 at room temperature. Polymers were heated to the melt, annealed for 10 min and subsequently cooled to 30 °C at 20 °C min^{-1}. The data represent the *d*-spacings in Å.

All these characteristic IR-bands are located at almost exactly the same wave numbers as in the IR-spectra of the bisamide-diol (2) monomer [31]. The bisamide-diol (2) monomer showed IR-bands at 1559, 1474, 1422, 686 and 590 cm^{-1} belonging to the amide II, NH vicinal CH_2 bend, CO vicinal CH_2 bend, amide V and VI, respectively. From these results and the WAXD data [31], it was found that bisamide-diol (2) consists of a mixture of α-and γ-type crystals and it thus seems that the crystalline structures are preserved in PEA(2) 49/51.

The WAXD spectra of the poly(ester amide)s (Fig. 3) confirm the conclusion that different type of crystalline phases are present. PEA(4) 44/56 shows two broad reflections at 3.94 and 4.34 Å and these reflections are characteristic of the α-crystalline phase as present in nylon 6,6 (4.4 and 3.7 Å). These reflections represent the distance between two amide–amide intermolecular H-bonded chains (4.4 Å) and the distance between two van der Waals packed sheets (3.7 Å). In the α-crystalline phase polymer chains are in an extended zig-zag planar conformation and H-bonds are formed between adjacent chains that make up a sheet. These H-bonded sheets are stacked upon each other and held together by van der Waals forces. The WAXD spectrum of the PEA(2) 49/51 polymer shows a broad peak with a *d*-spacing of ~4.1 Å similar to a γ-crystalline phase as present in nylon 6. In such a γ-type crystalline phase the amide groups are tilted with respect to the chain axis and H-bonds are formed within the sheets, between parallel chains. It can be concluded, similarly as from the FT-IR data, that PEA(2) 49/51 mainly crystallizes in a γ-type crystalline phase. However, also the presence of α-type crystals cannot be excluded in PEA(2) 49/51, because the resolution of the WAXD spectrum is too low. Care should be taken because a *d*-spacing of ~4.2 Å is also typical for the structure of aliphatic polyesters.

3.2. Thermal properties

The thermal stability of the segmented poly(ester amide)s under non-oxidative conditions was investigated by thermal gravimetric analysis. The decomposition temperature, taken at the inflection point, is ~375 °C for the PEA(4) polymers and ~400 °C for the PEA(2) polymers. Thus for all polymers the decomposition temperatures are considerably higher than the melting temperatures, which is necessary to process these materials by compression moulding.

The thermal properties of the poly(ester amide)s were determined by DSC. The crystallization and melting

temperatures and corresponding enthalpies of the polymers, obtained from the first cooling and second heating scan, are reported in Table 2. All polymers show two endothermic transitions denoted as $T_{m,1}$ and $T_{m,2}$ for the low and high melt transition, respectively. These transitions in the poly(ester amide)s are ascribed to the melting of crystals comprising single ester amide (EA) sequences ($T_{m,1}$) and crystals comprising two or more EA sequences ($T_{m,2}$).

Upon cooling from the melt, the polymers with 25 mol% hard segment show an exothermic transition at ~35 °C (Fig. 4). At this transition PEA(4) 72/28 and PEA(2) 74/26 crystals comprising single EA sequences are predominantly formed. Upon reheating PEA(4) 72/28 and PEA(2) 74/26 show an endothermic transition ($T_{m,1}$) between 62 and 70 °C, followed by a recrystallization exotherm and a second melt transition ($T_{m,2}$) (Fig. 5). This exotherm can be ascribed to rearrangement of crystals into a more stable crystalline structure. Compared to PEA(4) 72/28, the transitions at $T_{m,1}$ and $T_{m,2}$ are broader and at a lower temperature for PEA(2) 74/26 which might be explained by melting of a mixture of α- and γ-type crystals at the transitions $T_{m,1}$ as well as $T_{m,2}$. The presence of this mixture of crystals probably suppresses the formation of well-defined crystals.

During cooling, PEA(4) 44/56 shows a multi modal transition which indicates that not only a crystalline phase containing single EA sequences is formed but also a crystalline phase comprising longer EA sequences. PEA(2) 49/51 shows two distinct exothermic transitions at 42 ($T_{c,1}$) and 86 °C ($T_{c,2}$) (Fig. 4). At T_{c2}, PEA(2) 49/51 crystallizes into a phase existing of two or more EA sequences and at $T_{c,1}$ PEA(2) 49/51 crystallizes into a phase comprising single EA sequences. Upon reheating PEA(4) 44/56 and PEA(2) 49/51 show an endothermic transition ($T_{m,1}$) at 67 and 62 °C, respectively, followed by a second melt transition ($T_{m,2}$) (Fig. 5). The $T_{m,2}$ is 126 and 130 °C for PEA(4) 44/56 and PEA(2) 49/51, respectively. Moreover the transitions at $T_{m,1}$ and $T_{m,2}$ are broader for the PEA(2) than the PEA(4) copolymers. This can be attributed to melting of a mixture of α- and γ-type crystals (vide supra) present in the PEA(2) copolymers.

Previous work has shown that the $T_{m,2}$ and the corresponding enthalpies of the PEA(4) polymers are dependent on the polymer hard segment content [30]. By increasing the amount of hard segment in the polymer the fraction of hard blocks comprising two or more EA sequences increases resulting in an increase in $T_{m,2}$ (lamellar thickness) and $\Delta H_{m,2}$. The number average EA sequence length k, calculated with a probability function, increases from 1.4 for PEA(4) 72/28 to 2.2 for PEA(4) 44/56 [36]. Statistically, about 50% of all EA segments are present as single units in poly(ester amide)s with 25 mol% of amide content. In the poly(ester amide)s with 50 mol% of amide content about 20% of all EA segments are present as single units, whereas 80% have EA sequence lengths of two or more. This is reflected in the much lower $\Delta H_{m,2}$ of PEA-25 polymers compared to PEA-50 polymers. The crystallinity of the PEA-25 polymers was approximately 12.5±2.5% and that of the PEA-50 polymers 27.5±2.5% (Table 3).

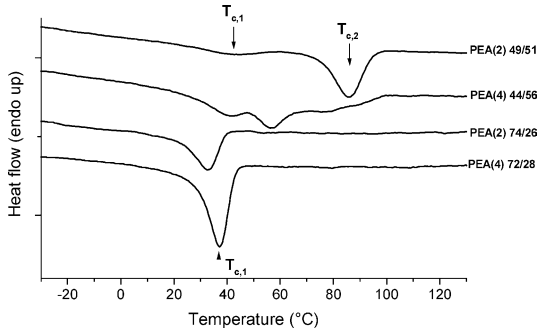

Fig. 4. DSC cooling scans (20 °C min^{-1}) of PEA(4) and PEA(2) polymers.

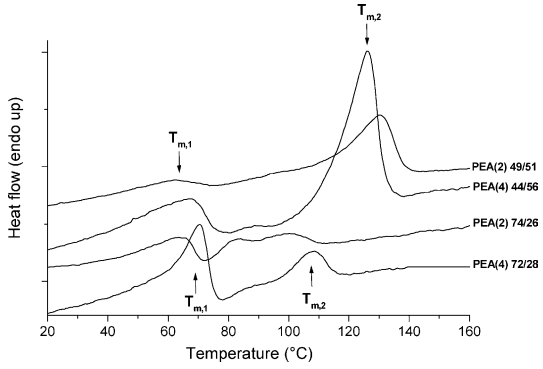

Fig. 5. DSC heating scans of PEA(4) and PEA(2) polymers, after cooling at a rate of 20 °C min^{-1}.

3.3. Dynamic mechanical properties

The flow temperature, as obtained from DMA

Table 2
Thermal properties of PEA(4) and PEA(2) polymers

Polymer code	$T_{m,1}$ (°C)	$\Delta H_{m,1}$ (J g^{-1})	$T_{c,1}$ (°C)	$\Delta H_{c,1}$ (J g^{-1})	$T_{m,2}$ (°C)	$\Delta H_{m,2}$ (J g^{-1})	$T_{c,2}$ (°C)	$\Delta H_{c,2}$ (J g^{-1})
PBA					63	58	24	−57
PEA(4) 72/28	70	24	–	–	108	9	37	−23
PEA(2) 74/26	64	9	–	–	75–110[a]	8	33	−14
PEA(4) 44/56	67	16	–	–	126	32	40/56/79[b]	−34
PEA(2) 49/51	62	5	42	−5	130	25	86	−18

[a] Melting range.
[b] Trimodal.

Table 3
Thermal properties of PEA(4) and PEA(2) polymers as obtained from DMA and DSC

Polymer code	Hard segment x (mol%)	T_{flow}[a] (°C)	$T_{m,2}$[b] (°C)	w_c[c] (%)	$G'_{25\,°C}$[a] (MPa)	T_g[a] (°C)
PEA(4) 72/28	28	105	108	12.5±2.5	62	−40
PEA(2) 74/26	26	94	75–110[d]	12.5±2.5	51	−40
PEA(4) 44/56	56	130	126	27.5±2.5	103	−20
PEA(2) 49/51	51	130	130	27.5±2.5	103	−25

[a] From DMA.
[b] From DSC.
[c] Crystallinity according to amide I band in FT-IR spectra.
[d] Melting range.

measurements, was similar to $T_{m,2}$, for all polymers (Table 3). All poly(ester amide)s show a transition in the rubber plateau (Fig. 6), which is found at temperatures corresponding with the lower melting temperature ($T_{m,1}$, Table 2).

The storage modulus (G') is a measure for the overall crystallinity of the polymers. The G' at 25 °C is ~50–60 and 103 MPa for the PEA-25 and PEA-50 polymers, respectively, indicating a similar crystallinity for PEA(2) and PEA(4) polymers.

Only glass transition temperature (T_g) data obtained by DMA measurements are presented in Table 3 since DSC traces only showed very weak transitions at the polymer T_g, which made their evaluation rather inaccurate. Similar T_gs were found for the PEA(2) and PEA(4) polymers as was expected because a similar concentration of amide segments is present in the amorphous phase.

3.4. Mechanical properties

Typical stress–strain curves of PEA(2) and PEA(4) polymers are presented in Fig. 7. The stress–strain curves of poly(ester amide)s show a yield stress followed by strain softening, necking and stabilisation of the neck [30].

Increasing the hard segment content in the PEA(4) and PEA(2) polymers results in an increase of the elastic modulus, yield stress and stress at break as was expected because of the increased stiffness (Table 4). The polymers have a strain at break between ~600 and 800%.

The PEA(2) and PEA(4) polymers have comparable tensile properties, although the stress at break is lower and strain at break is higher for PEA(4) 72/28 compared to PEA(2) 74/26. However, it should be taken into account that the stress and strain at break are sample properties rather than material properties. Apparently, the different crystalline structures (α- or γ-type) of the polymers have hardly any influence on their tensile properties.

The compression set (CS) at room temperature (Table 4) was measured to determine the elasticity of the poly(ester amide)s. At 25% compression the poly(ester amide)s are strained above the yield point. Previous work has shown that the compression set of PEA(4) polymers increased with increasing hard segment content up to a hard segment content of 50 mol% [30]. Likewise, the compression set is increasing from 12 to 24% with increasing hard segment for the PEA(2) polymers. However, the compression set of the PEA(2) polymers is substantially lower compared to the PEA(4) polymers. As the crystallinity and the morphology of PEA(4) and PEA(2) polymers with the same hard segment content is similar, the elastic recovery was expected to be the same. However, the visco-elastic recovery process of the PEA(4) and PEA(2) may differ significantly in time. If the recovery time, e.g. the time after the load was released, would have been extended the compression set values might be much closer together.

3.5. Water uptake

The water absorption of poly(ester amide) samples,

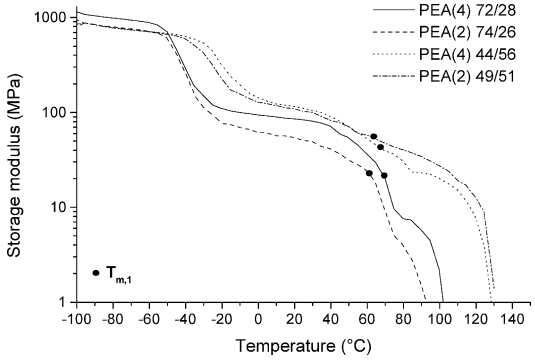

Fig. 6. Storage modulus as a function of temperature for PEA(4) and PEA(2) polymers.

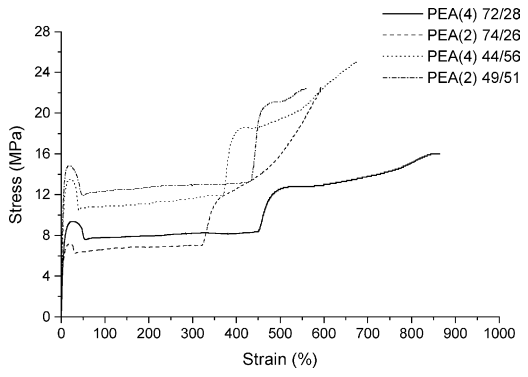

Fig. 7. Stress strain curves for PEA(4) and PEA(2) polymers.

Table 4
Mechanical properties of PEA(4) and PEA(2) polymers

Polymer code	E[a] (MPa)	σ_{yield} (MPa)	$\sigma_{at\ break}$ (MPa)	$\varepsilon_{at\ break}$ (%)	ε_{yield} (%)	$CS_{25\%}$ (%)
PEA(4) 72/28	180±36	9±0.5	15±1.0	810±100	24±1	39±5
PEA(2) 74/26	159±27	7±0.2	23±0.5	600±10	20±1	12±5
PEA(4) 44/56	270±42	14±0.5	25±1.0	680±30	18±1	49±6
PEA(2) 49/51	359±20	15±0.5	22±1.5	590±90	16±1	24±6

[a] E modulus only indicate a trend.

immersed in water at 37 °C, was followed in time over a period of 3 weeks. The polymers show an increase in water absorption in time, which levels off at 2–3 days (equilibrium). In Table 5 the water uptake at equilibrium is listed for the PEA(4) and PEA(2) polymers.

The water absorption for the PEA(4) polymers increased with decreasing hard segment content. However, the water absorption of the PEA(2) polymers is low and seems independent of the hard segment content. From literature it is known that water uptake takes place exclusively in the amorphous regions. Polymers PEA(4) and PEA(2) with the same hard segment content (and thus crystallinity) are thus expected to have a similar water uptake. From IR-data it was concluded that PEA(4) and PEA(2) polymers both have amide–amide H-bonds present in the disordered amorphous phase. PEA(2) polymers mainly have a γ-type crystalline structure which is characterized by fully (linear) H-bonded structure which is more stable (shorter H-bonds) compared to the α-type crystalline structure. It is assumed that H-bonds in the amorphous phase of PEA(2) are also shorter and thus stronger compared to those of PEA(4). The more compact H-bonds of PEA(2) are thus less accessible for solvation by water molecules. Water molecules might also be involved in breakage of the H-bonds between the amide–amide and ester–amide groups. This breakage is expected to be more difficult for the stronger H-bonds in the amorphous phase of PEA(2).

4. Conclusions

Segmented poly(ester amide)s were prepared by melt polycondensation of dimethyl adipate, 1,4-butanediol and a symmetrical bisamide-diol with 2 or 4 methylene units between the amide groups, abbreviated as PEA(2) and PEA(4), respectively. All polymers have a sub-ambient glass transition temperature and two melt transitions, corresponding with the melting of crystals comprising single ester amide sequences or two or more ester amide sequences. The poly(ester amide)s have a micro-phase separated structure with an amide-rich hard phase and an ester-rich flexible soft phase and crystallize into an α- or a γ-type crystalline phase, similar to α- or γ-crystals present in nylons. PEA(4) polymers crystallize into an α-type crystalline phase, while a mixture of α- and γ-type crystalline phases was found for PEA(2) polymers. In the IR- and WAXD-spectra of the bisamide-diol monomer α- and γ-related bands were found which indicates that the crystalline structures present in the monomer are preserved in the corresponding poly(ester amide). The polymers have an elastic modulus in the range of 159–359 MPa, a stress at break in the range of 15–25 MPa combined with a high strain at break (590–810%). The thermal and mechanical properties are not influenced by the different crystalline structures of the polymers, only by the amount of crystallizable hard segment present. However, the compression set and water absorption are significantly lower for the PEA(2) polymers compared to PEA(4) polymers.

Table 5
Equilibrium water uptake of PEA(4) and PEA(2) polymers, immersed in water at 37 °C

Polymer code	$Time_{equilibrium}$ (days)	Water $uptake_{37\ °C}$ (%)
PEA(4) 72/28	3	11.7±0.1
PEA(2) 74/26	2	4.4±0.1
PEA(4) 44/56	2	9.4±0.1
PEA(2) 49/51	2	4.2±0.2

Acknowledgements

DOW Benelux N.V. is acknowledged for the synthesis of N,N'-1,2-ethanediyl-bis[6-hydroxy-hexanamide]. This study was financially supported by the European Commission, project: QLK5-1999-01298.

References

[1] Alla A, Rodríguez-Galán A, Martínez de llarduya A, Muñoz-Guerra S. Polymer 1997;38(19):4935–44.
[2] Andini S, Ferrara L, Maglio G, Palumbo R. Macromol Chem Rapid Commun 1988;9:119–24.
[3] Asín L, Armelin E, Montané J, Rodríguez-Galán A, Puiggalí J. J Polym Sci, Part A: Chem 2001;39:4283–93.
[4] Barrows TH. The design and synthesis of bioabsorbable poly(ester-amides). Polymers in medicine II. New York: Plenum; 1986.
[5] Bera S, Jedlinski Z. J Polym Sci, Part A: Polym Chem 1993;31(3):731–9.
[6] Botines E, Rodríguez-Galán A, Puiggalí J. Polymer 2002;43:6073–84.
[7] Castaldo L, de Candia F, Maglio G, Palumbo R, Strazza G. J Appl Polym Sci 1982;27:1809–22.
[8] de Candia F, Maglio G, Palumbo R. Polym Bull 1982;8:109–16.
[9] de Simone V, Maglio G, Palumbo R, Scardi V. J Appl Polym Sci 1992;46:1813–20.
[10] Fey T, Hölscher M, Keul H, Höcker H. Polym Int 2003;52:1625–32.

[11] Gomurashvili Z, Katsarava R. J Mater Sci, Pure Appl Chem 2000; A37(3):215–27.
[12] Goodman I, Sheahan RJ. Eur Polym J 1990;26(10):1081–8.
[13] Katayama S, Murakami T, Takahashi Y, Serita H, Obuchi Y, Ito T. J Appl Polym Sci 1976;20:975–94.
[14] Goodman I, Starmer DA. Eur Polym J 1991;27(6):515–22.
[15] Katsarava R, Beridze V, Arabuli N, Kharadze D, Chu C, Won CY. J Polym Sci, Part A: Polym Chem 1999;37:391–407.
[16] Paredes N, Rodríguez-Galán A, Puiggalí J. J Polym Sci, Part A: Polym Chem 1998;36:1271–82.
[17] Qian ZY, Sai L, Hailian Z, Xiaobo L. Colloid Polym Sci 2003;281: 869–75.
[18] Rodriguez-Galan A, Vera M, Jiménez K, Franco L, Puiggalí J. Macromol Chem Phys 2003;204:2078–89.
[19] Villuendas I, Bou JJ, Rodríguez-Galán A, Muñoz-Guerra S. Macromol Chem Phys 2001;202(2):236–44.
[20] Stapert HR, Dijkstra PJ, Feijen J. Macromol Symp 2000;152:127–37.
[21] Stapert HR, Dijkstra PJ, Feijen J. Macromol Symp 1998;130:91–102.
[22] Stapert HR, Bouwens AM, Dijkstra PJ, Feijen J. Macromol Chem Phys 1999;200(8):1921–9.
[23] Bera S, Jedlinski Z. Polymer 1992;33(20):4331–6.
[24] Sudha JD. J Polym Sci, Part A: Polym Chem 2000;38:2469–86.
[25] Sudha JD, Pillai CKS, Bera S. J Polym Mater 1996;13(4):317–28.
[26] Katayama S, Horikawa H, Ito Y, Gomyo N, Obuchi Y. J Appl Polym Sci 1971;15:775–96.
[27] Barrows TH, Horton VL. Progress in biomedical polymers 1988. Proceedings American Chemical Society Symposium [Los Angeles].
[28] Castaldo L, Maglio G, Palumbo R. Polym Bull 1992;28:301–7.
[29] Pivsa-Art S, Nakayama A, Kawasaki N, Yamamoto N, Aiba S. J Appl Polym Sci 2002;85(4):774–84.
[30] Lips PAM, Broos R, van Heeringen MJM, Dijkstra PJ, Feijen J. Submitted for publication.
[31] Lips PAM, van Heeringen MJM, Broos R, Dijkstra PJ, Feijen J. To be published.
[32] Shroff RN. J Appl Polym Sci 1965;9:1547–51.
[33] Solomon OF, Ciuta IZ. J Appl Polym Sci 1962;6:683–6.
[34] Kricheldorf HR, Rabenstein M, Maskos M, Schidt M. Macromolecules 2001;34:713–22.
[35] Kricheldorf HR, Böhme S, Schwarz G. Macromolecules 2001;34: 8879–85.
[36] Cella RJ. J Polym Sci 1973;42:727–40.